

Editorial Manager(tm) for Medical & Biological Engineering & Computing
Manuscript Draft

Manuscript Number: MBEC848

Title: Simultaneous Determination of Wave Speed and Arrival Time of Reflected Waves Using the Pressure-Velocity loop

Article Type: Original article

Section/Category:

Keywords: wave speed; reflected waves; wave intensity analysis;
PU-loop

Corresponding Author: Dr Ashraf William Khir, PhD

Corresponding Author's Institution: Brunel University

First Author: Ashraf W Khir, PhD

Order of Authors: Ashraf W Khir, PhD; Marcel J Swalen, BSc; Jiling Feng, MSc; Kim H Parker, PhD

Manuscript Region of Origin:

Abstract: In a previous paper we demonstrated that the linear portion of the pressure-velocity loop (PU-loop) corresponding to early systole could be used to calculate the local wave speed. In this paper we extend this work to show that determination of the time at which the PU-loop first deviates from linearity provides a convenient way to determine the arrival time of reflected waves (T_r). We also present a new technique using the PU-loop that allows for the determination of wave speed and simultaneously.

We measured pressure and flow in elastic tubes of different diameters, where a strong reflection site existed at known distances away from the measurement site. We also measured pressure and flow measured in the ascending aorta of 11 anaesthetised dogs where a strong reflection site was produced through total arterial occlusion at 4 different sites. Wave speed was determined from the initial slope of the PU-loop and T_r was determined using a new algorithm that detects the sampling point at which the initial linear part of the PU-loop deviates from linearity.

The results of the new technique for detecting Tr were comparable to those determined using the foot-to-foot and wave intensity analysis methods. In elastic tubes Tr detected using the new algorithm was almost identical to that detected using wave intensity analysis and foot-to-foot methods with a maximum difference of 2%. Tr detected using the PU-loop in vivo highly correlated with that detected using wave intensity analysis ($r^2=0.83$, $P < 0.001$).

We conclude that the new technique described in this paper offers a convenient and subjective method for detecting Tr, and allows for the dynamic determination of wave speed and Tr, simultaneously.

Suggested Reviewers: Nicos Westerhof
n.westerhof@vume.nl

Juin-Jr Wang
jjwang@ucalgary.ca

Jos Spaan
j.a.spaan@amc.uva.nl

Patrick Segers
patrick.segers@ugent.be

Simultaneous Determination of Wave Speed and Arrival Time of Reflected Waves Using the Pressure-Velocity loop

Khair AW¹, Swalen MJP¹, Feng J¹ and Parker KH²

¹ Brunel Institute for Bioengineering & the School of Engineering and Design

Brunel University, Uxbridge, Middlesex, UK.

² Physiological Flow Studies Group, Department of Bioengineering, Imperial College

London, South Kensington, UK.

Running title: wave speed and the arrival time of reflected waves

Corresponding Author:

Dr Ashraf Khir

Brunel institute for Bioengineering

Brunel University

Uxbridge

Middlesex UB8 3PH

UK

Tel: +44 1895265857

Fax: +44 1895274608

Email: Ashraf.khir@brunel.ac.uk

Abstract

In a previous paper we demonstrated that the linear portion of the pressure-velocity loop (PU-loop) corresponding to early systole could be used to calculate the local wave speed. In this paper we extend this work to show that determination of the time at which the PU-loop first deviates from linearity provides a convenient way to determine the arrival time of reflected waves (Tr). We also present a new technique using the PU-loop that allows for the determination of wave speed and simultaneously.

We measured pressure and flow in elastic tubes of different diameters, where a strong reflection site existed at known distances away from the measurement site. We also measured pressure and flow measured in the ascending aorta of 11 anaesthetised dogs where a strong reflection site was produced through total arterial occlusion at 4 different sites. Wave speed was determined from the initial slope of the PU-loop and Tr was determined using a new algorithm that detects the sampling point at which the initial linear part of the PU-loop deviates from linearity.

The results of the new technique for detecting Tr were comparable to those determined using the foot-to-foot and wave intensity analysis methods. In elastic tubes Tr detected using the new algorithm was almost identical to that detected using wave intensity analysis and foot-to-foot methods with a maximum difference of 2%. Tr detected using the PU-loop *in vivo* highly correlated with that detected using wave intensity analysis ($r^2=0.83$, $P < 0.001$).

We conclude that the new technique described in this paper offers a convenient and subjective method for detecting Tr, and allows for the dynamic determination of wave speed and Tr, simultaneously.

Key words: wave speed, reflected waves, wave intensity analysis, PU-loop

Introduction

The arrival time of reflected waves to the root of the aorta is of physiological importance (27). If the reflected compression waves arrive before the aortic valve is closed, the left ventricle will be required to produce extra work to overcome the increase in pressure associated with those reflected waves (8). The arrival time of reflected waves depends principally on the distance to the sites of reflection and on wave speed; the higher the wave speed the earlier the arrival time of reflected waves.

Several methods have been proposed to identify the arrival time of reflected waves. Westerhof et al. (29) used the input impedance to calculate the distance to the nearest reflection site, from which, they determined the arrival time of reflected waves. Van Den Bos et al. (28) introduced a method for determining the arrival time of reflected waves based on the time delay between the forward and backward components of the pressure waveform. Murgo et al. (20) suggested that the temporal time from the initial pressure upstroke to the pressure inflection point is the time that it takes the wave to run forward, be reflected and arrive back. With knowledge of the wave speed the distance to reflection site can be determined. More recently, Pythoud et al. (25) proposed the “reflection profile” method to determine the distances of the most important reflection sites by deconvoluting the backward pressure wave. Parker et al. (23) introduced wave intensity analysis (WIA) for studying travelling waves in arteries. The method allows for the separation of waves into their forward and backward directions (24) and because WIA is a time-domain analysis, the arrival of the reflected waves to the measurement site is readily available in the results of this analysis as the onset of the backward wave. The accuracy of WIA has been tested *in vitro* (11), used *in vivo* in animal models (12,26) and has also been used for detecting the arrival time of reflected waves in patients (10,13). The determination of the arrival time of the reflected

waves using any of the above methods requires knowledge of the wave speed, which can be measured using any of the methods summarised in the following paragraphs.

Wave speed measurements can generally be grouped under two main categories, spatial and local techniques. Spatial wave speed in the arterial system has been predominantly obtained using the foot-to-foot method which entails measuring either pressure or flow waveforms at two sites that are at a known distance apart, L . Dividing L by the time it took the wave to run from one site to the other, Δt , gives wave speed, $c = \frac{L}{\Delta t}$. This method has been used extensively and the results confirm that the wave speed along the aorta is not uniform; a significant increase is observed distally (14,18,21). Although this method is being used clinically and in a number of epidemiological studies (1,6,19) the non-invasive results are somewhat controversial and subjective because of the difficulty in determining the foot of the wave with sufficient accuracy and because of the difficulty in measuring the distance between the two measurement sites due to the curvature of the arteries (7).

Local wave speed refers to the determination of wave speed at the measurement site. Westerhof *et al.* used the characteristic impedance to give an estimate of local wave speed (28) and Davies *et al.*, introduced a new technique for determining local wave speed also based on the measurements of pressure and flow at the same site (4). In a previous paper we introduced the PU-loop method for determining local wave speed (9). The method is based on the water hammer equation which states that, if waves at the measurement site are running only in one direction, the relationship between pressure and velocity is linear. Therefore, during the early part of systole it is most probable that only forward waves are present in the ascending aorta and the initial slope of the PU-loop is directly related to wave speed. A consequence of this is that the arrival of a reflected wave will change the relationship between pressure and velocity from the linearity that exists when only forward waves are present. The PU-loop becomes nonlinear after the arrival of reflected wave.

We therefore hypothesise that the end of the initial linear part of the PU-loop during early systole marks the arrival time of reflected waves. Hence, the main objectives of this paper are: a) to present a new technique to test this hypothesis, and b) to demonstrate the simultaneous determination of the initial linear slope of the PU-loop indicating wave speed, and detecting the point of deflection at the end of this linear part indicating the arrival time of reflected waves.

Materials and Methods

The pulse wave speed and the arrival time of the reflected waves were determined in two sets of data; *in vitro* and *in vivo*.

***In vitro* experiments**

A schematic diagram of the experimental setup is shown in **Figure 1** and a description of the individual elements follows.

The pump: A positive displacement syringe pump was used to generate an approximately half-sinusoidal pulse wave. The pump consists of a cylinder and a piston that is driven by an electric motor running at a constant speed (Maxon, Sachseln, Switzerland). The cylinder of the pump is 5cm in diameter and the linear movement of the piston is 2cm, giving a displaced volume of approximately 40ml. In all of the experiments we generated and analysed a single half-sinusoidal pulse, in which the piston moved forward from its bottom to top dead centre positions.

Tubes: We used flexible tubes made of latex (3S Health Care, London, UK). Tubes were uniform along their lengths with a circular cross sectional area and were obtained with a standard length of 100 cm. We used tubes with 4, 8 and 16mm unstressed diameter with wall thickness approximately 0.25mm.

To eliminate gravitational and contact stresses between the elastic tubes and any hard surfaces during the experiments, the tube was immersed in an open tank containing tap water.

The tubes were able to extend and distend freely and were fully immersed, where the level of water above the surface of the tube was approximately 1cm. We note that the transmural pressure will vary for the different sized tubes, however this variation is ignored as the difference is insignificant. We also note that there will be a hydrostatic pressure difference between the top and bottom surfaces of the latex tube, however its value is considerably smaller than mean pressure in the tube. We expect its effect to be minimal, and so ignored it.

The outlet of each tube was attached to a hard plastic connector (Portex) of a matching size. The Portex connector was attached to a relatively rigid, thick-walled polyurethane tube that was connected to the downstream reservoir, which is made of hard plastic. The outlet of each tube was considered a strong reflection site because of the hard connector and rigid tubing. An upstream reservoir was connected to prevent pump cavitations and air bubbles entering the system.

Measurements: Pressure and flow-rate were recorded simultaneously at different locations along each tube, which are detailed as shown in **Table 1**. Pressure was measured using a 6F catheter with a strain gauge pressure transducer (Gaeltec, Scotland, UK), which was advanced to the measurement site through a Y connector at the inlet of the tube. Flow-rate was measured using an ultrasound flow meter and an ultrasound flow probe (Transonic, Ithaca, NY, USA), which fits snugly to each tube. The pressure catheter was calibrated against a column of water with a variable height, and the ultrasound flow probes were calibrated against the preset calibration signals of the flow meter. Data were sampled at a frequency of 500 Hz using Labview (National Instruments, TX, USA), and were subsequently analysed using programs prepared in Matlab (The Mathworks Inc, Ithaca, NY, USA).

In vivo experiment

Animal preparations: This study, which conformed to the “Guiding Principles of Research Involving Animals and Human Beings” of the American Physiological Society, was performed in 11 mongrel dogs (average weight 22 ± 3 kg, 7 males). Animals were anaesthetised with sodium pentobarbital, 30 mg/kg-body weight intravenously, and a maintenance dose of 75 mg/hr was given intravenously for the duration of the experiment. Each dog was endotracheally intubated and mechanically ventilated using a constant-volume ventilator (Model 607, Harvard Apparatus Company, Millis, MA., USA). After a median sternotomy, an ultrasonic flow probe (Transonic Systems Inc., Ithaca, N.Y., USA) was mounted around the ascending aorta approximately 1 cm distal to the aortic valve. ECG leads were connected to both forelegs and the left back leg. A high-fidelity pressure catheter (Millar Instruments Inc., Houston, Texas, USA) was used to measure the pressure in the aortic root as near as possible to the site of the flow probe without creating interference (a few millimetres away from the flow probe, proximal to the aortic valve). The pressure catheter was advanced from either the right or the left brachial artery. Snares were placed at 4 different sites during the preparation of each dog: the upper descending thoracic aorta at the level of the aortic valve (thoracic); the lower thoracic aorta at the level of the diaphragm (diaphragm); the abdominal aorta between the renal arteries (abdominal) and the left iliac artery, 2 cm downstream from the aorta-iliac bifurcation (iliac).

Protocol: For each occlusion, data were collected for 30 seconds before the occlusion (control) and during the occlusion; 3 minutes after the snare was applied¹. At each site, total occlusion was confirmed by observing no flow distal to the occlusion site, and another Millar high-fidelity pressure catheter was advanced from either the right or left iliac artery to

measure pressure at the occlusion site. A time interval of 10-15 minutes was allowed between occlusions to return to control conditions. In order to eliminate effects due to the cumulative time of the procedure, the sequence of occlusions was varied from dog to dog using a 4 by 4 Latin-square. The circumference of the *post-mortem* ascending aorta was measured to convert the measured flow rate into velocity. We note that the circumference of the ascending aorta of each dog was measured at zero transmural pressure and hence the calculated diameter may be less than the actual diameter *in vivo*. However, In order to compensate for that difference, we did not take into account the wall thickness and assumed that the measured external radius is the correct value to be used in calculating the velocities (12). To eliminate the effect of the possible time lag attributable to the filter in the ultrasonic flow meter, the foot of the pressure and velocity waveforms were aligned at the onset of ejection, as previously described (9), and the lag was accounted for prior to carrying out the analysis.

The pressure catheters were calibrated prior to each experiment against a mercury manometer. All *in vivo* data were recorded at a sampling rate of 200 Hz, stored digitally and were analysed using Matlab software (The MathWorks Inc., Natick, Mass, USA).

Regression analyses were performed to identify the correlation factor and its significance. Values of $p < 0.05$ were considered significant. The Bland-Altman (2) technique was used to establish whether there was a significant difference between the results of the new technique and those of WIA. The acceptable range for the mean difference was taken as \pm double standard deviation.

Analysis

Three methods to determine the arrival time of the reflected waves have been used: the foot-to-foot, WIA and the PU-loop.

Foot-to-foot

As discussed above, the foot-to-foot method is traditionally used for calculating wave speed. However, if the wave speed (c), and the distance between two measurement sites (L) is known, the relative arrival time of the reflected waves can be determined as $\Delta t = \frac{2L}{c}$, which is the time it takes the wave to run from one site to the other, be reflected and run back to the measurement site. This method has been used in the *in vitro* study only.

Wave intensity analysis

The theoretical basis of WIA is the solution of the classical 1-D conservation of mass and momentum equations and the derivation of the following equations is found in earlier papers (22,23). The net wave intensity, dI , is calculated as $dI = dP dU$, where dP and dU are respectively the pressure and velocity differences over one sampling period. The pressure and velocity differences across the measured wavefronts are assumed to be the addition of the differences across the forward (+) and backward (-) pressure and velocity wavefronts; $dP = dP_+ + dP_-$ and $dU = dU_+ + dU_-$. This assumption enables us to write the intensities of the forward and backward waves

$$dI_{\pm} = \pm \frac{1}{4\rho c} (dP \pm \rho c dU)^2 \quad (1)$$

Where ρ is density and c is wave speed which was determined using the PU-loop method (8). We note that wave intensity has the useful characteristics that it is positive for forward waves and negative for backward waves. Therefore, the relative arrival time of reflected waves was determined as the time of the first sampling points when dI . (the backward intensity) was

substantially bigger than the noise level determined from the initial part of the dI curve. This method has been used in both the *in vitro* and *in vivo* studies.

PU-loop

The theoretical basis of the PU-loop method for determining wave speed is the water hammer equation, which can be written for the forward and backward waves as

$$dP_{\pm} = \pm \rho c dU_{\pm} \quad (2)$$

Equation (2) describes the relationship between changes in the pressure and velocity, and plotting the measured pressure against the measured velocity over the cycle we obtain a PU-loop. During the very early part of the cycle when only forward waves are expected to be present, the slope of the PU-loop should be linear. On arrival of the reflected waves, the linear relationship between pressure and velocity will no longer hold and there will be a deflection point, after which the loop becomes non-linear. The slope of the PU-loop, S , during any time interval is $S = \frac{dP}{dU}$. We define $t=0$ as the time of the foot of the initial pressure waveform, and $t=t_r$ as the time at which the reflected wave returns to the site of measurement.

When $t < t_r$, and only forward waves are present, the slope of the initial linear part of the loop

$$\text{is } S_0 = \frac{dP_+}{dU_+} = \rho c \quad (3)$$

When the reflected wave arrives back to the measurement site, and both forward and backward waves are present, the slope at $t = t_r$ can be written

$$S_r = \frac{dP}{dU} = \rho c \frac{dP_+ + dP_-}{dP_+ - dP_-} \quad (4)$$

Calculating the relative change in slope, ΔS , at $t = t_r$ gives

$$\Delta S = \frac{S_r - S_0}{S_0} = \frac{2dP_-}{dP_+ - dP_-} \quad (5)$$

When ΔS was greater than a threshold, τ , the initial part of the PU-loop was deemed no

longer linear and the time of that interval is considered the arrival time of the reflected wave.

The optimal value of τ was determined by trial-and-error and found to be $\tau = 0.35$.

A program was written in MatLab (MathWorks Inc, Natick, Mass, USA) to automate the determination of the linear part in the *PU*-loop and to detect the sampling point at which the loop deviates from linearity, which we hypothesise to be the arrival time of reflected

waves. The program calculates the local slope, S_i , at each sampling time $S_i = \frac{P_{i+1} - P_i}{U_{i+1} - U_i}$,

where P_i and U_i are the pressure and velocity at time t_i . To find the end of the initial linear part of the *PU*-loop, denoted by point R in **Figure 2**, the program calculates the relative difference between the current slope and the average of all the previous slopes starting from the beginning of the linear part, point K.

$$\Delta S_i = \frac{S_i}{\left(\frac{1}{i-K} \sum_{i=K}^{i-1} S_i \right)} - 1 \quad (6)$$

When $\Delta S_i \geq \tau$, the time of that interval is considered the arrival time of the reflected wave.

This algorithm is a point-to-point technique and the program analyses one interval at a time. The program starts the analysis at the foot of the pressure waveform, which is the beginning of the linear part, proceeds to find the end of the linear part indicating the arrival time of reflected waves, and simultaneously determines the slope of the initial linear part indicating wave speed, then it stops. This method has been used in both the *in vitro* and *in vivo* studies.

Results

In vitro experiment

For each of the three tubes, 3 measurements were taken at three distances; 30, 40 and 50cm away from the reflection site. The time of arrival of the first reflected wave was determined for each case, using 3 methods: the new technique utilising the PU-loop, WIA and the foot-to-foot method. The arrival time of reflected waves detected using the PU-loop method *in vitro*, point R, was highly correlated with that detected using the foot-to-foot-method ($r^2=0.97$, $p<0.001$) and the WIA, point M, ($r^2=0.95$, $p<0.001$). **Fig. 2** shows that the time of the sampling point at the end of the linear part of the *PU*-loop as determined by the new algorithm, and the onset of reflection as determined by wave intensity, occur almost simultaneously. This was found to be true in all of the cases that we tested. Times of arrival of the reflected wave to the different measurement sites in the different size tubes using the three methods are given in **Table 1**. The maximum difference between the arrival time of reflected waves determined by the new algorithm and both other methods was approximately 2%, which occurred in the 16mm diameter tube.

In vivo experiment

Figure 3 and **Figure 4** show the time of the sampling point at the end of the linear part of the *PU*-loop as determined by the new algorithm, point R, and the onset of reflection as determined by wave intensity, point M, during control and during thoracic occlusion respectively. During occlusion the strong reflection site results in a strong reflected wave that is marked by a clear deflection point on the *PU*-loop, point R, as shown in **Figure 4**. Although the end of the initial linear part of the *PU*-loop during control is less obvious than that during occlusion, the new technique accurately detects the time of arrival of reflected waves as detected by WIA in both cases. The arrival time of reflected waves determined by the *PU*-

loop during all occlusions correlated well with that determined by the WIA ($r^2=0.83$, $p<0.001$), as shown in **Figure 5a**.

We used the Bland-Altman plot to compare the results of the WIA and the PU-loop methods for determining the arrival time of reflected waves. The mean value of the difference between the results of the two methods was 0.003 and the standard deviation of that mean was ± 0.004 . As shown in **Figure 5b** most of the data points, as well as the zero line fell within the confidence range of the average, double the standard deviation ($\pm 2SD$) of the difference, indicating no statistical difference between the results of the two methods.

Discussion

In our earlier work we established that the linear portion of the PU-loop corresponding to early systole could be used to calculate the local wave speed (9). In this paper we extended this work and demonstrated that the time at which the initial part of the PU-loop first deviates from linearity provides a convenient way to determine the time of arrival of the reflected wave. Using the technique described in this paper allowed for the simultaneous determination of wave speed and the arrival time of reflected waves.

The program

As discussed in the analysis, the threshold τ , determines the accuracy of the linear part and represents the minimum allowed relative difference between slopes. We initially tested the algorithm and found by trial-and-error that $\tau=0.35$ is the value that gave the best results with *in vitro* data. The same value of τ has also given the best results with *in vivo* data. Since the *in vivo* data was collected at 200 Hz and the *in vitro* data at 500 Hz, it seems that the threshold is most likely sample rate independent.

To make sure the initial linear part of the PU-loop is not detected within the noise level, the length of the linear part was calculated and had to be at least 20 ms long before it was acceptable. The value of 20 ms has also been determined by trial and error and gave the best results in both the *in vivo* and *in vitro* data. If the length of the linear part is below this value, the program assumes the found linear part is within the noise level and continues searching for real linear part. Further, this technique has also been tested using these values of τ and the minimum length of the linear part with other data that are not presented here but was recorded at 1 kHz and also gave the best results. Therefore we found these values to be optimal in our experiments, and anticipate they could be suitable for analysing similar data that are recorded at sampling frequencies in the range of 200Hz to 1kHz.

Wave speed

Wave speed is an important property of an arterial segment and directly related to its compliance. Wave speed has been long used as a surrogate marker for aortic stiffness, which has recently been thought of as an independent predictor of stroke (16), cardiovascular mortality (15) in hypertensive patients. Aortic stiffness has also been associated with the reduction of coronary flow (17). Thus, automating the determination of wave speed is of clinical relevance and the results of this paper are encouraging towards achieving this aim. The PU-loop method is easy to use but requires the simultaneous measurements of pressure and flow velocity at the same site. We note that Dujardin and Stone used a similar loop (the flow-pressure loop) to determine the characteristic impedance (3).

The wave speed determined by using the PU-loop is traditionally made by establishing the slope of the initial part of the loop by eye. The new algorithm allows for automating this process, making the determination of wave speed by the PU-loop subjective. The average difference between the results of wave speed determined by eye and that determined automatically using this technique in the *in vivo* experiments, is in the order of 3% as shown in **Table 2**.

Because of the difficulty in obtaining accurate measurements of pressure non-invasively, other researchers have used a wall tracking system which allows for substituting pressure with vessel diameter (5). Harada *et al.* used an online technique for determining wave speed, and suggested that towards end of systole there may be another period where waves in the ascending aorta are also unidirectional, similar to the period at early systole. We anticipate the relationship between pressure and velocity at that time to also be linear, and if desired, the computer program implementing the algorithm in this paper can be adapted to detect other linear parts in the *PU*-loop. To do so, another search procedure is applied after

the first linear part has been detected and this algorithm can simply be used to detect other linear parts if needed.

Arrival time of reflected wave

Theoretically the end of the initial linear part of the PU-loop should occur at the same time as the onset of the first reflected wave determined using WIA. The comparison between the two methods is made to verify how well the new algorithm is able to detect the onset of nonlinearity between the pressure and velocity in the loop, which is regarded as the onset of reflected waves. As shown, the results of the new algorithm for the detection of the arrival time of the reflected waves are in agreement with those determined by both WIA and foot-to-foot methods, indicating the viability of the new technique. It is worth noting however that one of the limitations of this technique is that incorrect temporal alignment of pressure and velocity can influence the correct determination of the slope of the linear part, and thus the value of wave speed. Similarly, a time lag between the measurement of pressure and flow (or velocity) can introduce errors in the determination of the arrival time of the reflected wave.

The augmentation index (AIx) is used extensively clinically to quantify the magnitude of the reflected waves (22). The determination of AIx depends principally on detecting a change in the shape of the pressure waveform upon the arrival of the reflected waves using some derivative of the waveform (20); most authors used the 4th derivative. The accuracy of the technique depends upon the ability to detect an inflection point on the pressure waveform. However, in our experiments an inflection point in the pressure waveform was not always obvious as shown in the pressure waveforms in **Figure 3** and **4**. A comparison of the results of detecting the arrival time of the reflected wave between the method discussed in this paper and those used in establishing AIx has not been reported previously and it is a question for a separate study.

In Conclusion, the PU-loop method for determining local wave speed can also be used to detect the arrival time of reflected waves by identifying the end of the initial linear part of the loop. The proposed algorithm is most likely independent of sampling rate, and the results for calculating wave speed and determining the arrival time of reflected waves compare well with wave intensity analysis and foot-to-foot methods for calculating the same. The new technique offers a subjective method for determining the initial slope of the PU-loop indicating wave speed, and the end of the end of the linear part of the loop indicating the arrival time of reflected wave. The new algorithm utilising the PU-loop provides a new technique for the dynamic determination of wave speed and the arrival time of reflected waves simultaneously.

Acknowledgement: We would like to thank Professor JV Tyberg for offering the experimental facilities used to obtain the data. We also acknowledge the excellent technical support received from Ms. Rozsa Sas, Ms. Cheryl Meek and Mr. Gerald Groves.

References

1. **Asmar R, Rudnichi A, Blacher J, London GM, and Safar MF.** Pulse Pressure and Aortic Pulse Wave Are Markers of Cardiovascular Risk in Hypertensive Populations. *AJH* 14:91–9, 2001.
2. **Bland JM and Altman MG.** Statistical methods for assessing agreement between two methods of clinical measurement. *The Lancet*: 8;1(8476):307-310, 1986.
3. **Dujardin JP and Stone DN.** Characteristic impedance of the proximal aorta determined in the time and frequency domain: a comparison. *Med Biol Eng Comput* 19: 565-568, 1981.
4. **Davies JE, Whinnett ZI, Francis DP, Willson K, Foale RA, Malik IS, Hughes AD, Parker KH, and Mayet J.** Use of simultaneous pressure and velocity measurements to estimate arterial wave speed at a single site in humans. *Am J Physiol Heart Circ Physiol* **290**: H878-H885, 2006.
5. **Harada A, Okada T, Niki K, Chang D and Sugawara M.** On-line noninvasive one-point measurements of pulse wave velocity. *Heart Vessels*: 17:61-68, 2002.
6. **Jacques B, Asmar R, Djane S, London GM and Safar ME.** Aortic pulse wave velocity as a marker of cardiovascular risk in hypertensive patients. *Hypertension* 33:1111-1117, 1999.
7. **Karamanoglu M.** Errors in estimating propagation distances in pulse wave velocity. *Hypertension* 41:e8, 2003.
8. **Kelly RP, Tunin R, and Kass DA.** Effect of reduced aortic compliance on cardiac efficiency and contractile function of in situ canine left ventricle. *Circ Res* 71: 490-502, 1992.
9. **Khiri AW, O'Brien A, Gibbs S and Parker KH.** Determination of wave speed and wave separation in the arteries. *J Biomech* 34:1145-1155, 2001.

10. **Khiri AW, Henein MY, Koh T, Das SK, Parker KH and Gibson DG.** Arterial waves in humans during peripheral vascular surgery. *Clin Sc* 101: 749-757, 2001
11. **Khiri AW, and Parker KH.** Measurements of wave speed and reflected waves in elastic tubes and bifurcations. *J Biomech* 35: 775-783, 2002.
12. **Khiri AW and Parker KH.** Wave intensity in the ascending aorta: Effects of arterial occlusion. *J Biomech* 38: 647 -655, 2005.
13. **Koh TW, Pepper JR, DeSouza AC and Parker KH.** Analysis of wave reflections in the arterial system using wave intensity: a novel method for predicting the timing and amplitude of reflected waves. *Heart Vessels*: 13:103-113, 1998.
14. **Latham RD, Westerhof N, Spikema P, Rubal BJ, Reuderink P, and Murgo JP.** Regional wave travel along the human aorta: a study with six simultaneous micromanometric pressures. *Circ* 72: 1257-1269, 1985.
15. **Laurent S, Boutouyrie P, Asmar R, Gautier I, Laloux B, Guize L, Ducimetiere P and Benetos A.** Aortic stiffness is an independent predictor of all-cause and cardiovascular mortality in hypertensive patients. *Hypertension*: 37:1236-41, 2001.
16. **Laurent S, Katsahian S, Fassot C, Tropeano AI, Gautier I, Laloux B, Boutouyrie P.** Aortic stiffness is an independent predictor of fatal stroke in essential hypertension. *Stroke*: 34:1203-1206, 2003.
17. **Leung MC, Meredith IT and Cameron JD.** Aortic stiffness affects the coronary blood flow response to percutaneous coronary intervention. *Am J Physiol Heart Circ Physiol*:290(2):H624-630, 2006.
18. **McDonald DA.** Regional pulse-wave velocity in the arterial tree. *J Appl Physiol* 24: 73-78, 1968.
19. **McEniery CM, Yasmin, Hall IR, Qasem A, Wilkinson IB, Cockcroft JR; ACCT Investigators.** Normal vascular aging: differential effects on wave reflection and aortic

- pulse wave velocity: the Anglo-Cardiff Collaborative Trial (ACCT). *J Am Coll Cardiol* 46:1753-1760, 2005.
- 20. Murgo JP, Westerhof N, Giolma JP and Altobelli SA.** Aortic input impedance in normal man: relationship to waveforms. *Circ* 62:105-116, 1980.
- 21. Nichols WW and O'Rourke MF.** McDonald's Blood Flow in Arteries. 4th Ed., 1998. Edward Arnold, London.
- 22. Nichols WW.** Clinical measurement of arterial stiffness obtained from noninvasive pressure waveforms. *Am J Hypertens* 18: 3S-10S, 2005.
- 23. Parker KH, Jones CJ, Dawson JR, and Gibson DG.** What stops the flow of blood from the heart? *Heart Vessels* 4: 241-245, 1988.
- 24. Parker KH, and Jones CJ.** Forward and backward running waves in the arteries: analysis using the method of characteristics. *J Biomech Eng* 112: 322-326, 1990.
- 25. Pythoud F, Stergiopoulos N and Meister J-J.** Separation of arterial pressure into their forward and backward running components, *J Biomech Eng* 118: 295-301, 1996.
- 26. Sun YH, Anderson TJ, Parker KH, Tyberg JV.** Effects of left ventricular contractility and coronary vascular resistance on coronary dynamics. *Am J Physiol Heart Circ Physiol*: 286: H1590-595, 2004.
- 27. Ueda H, Hayashi T, Tsumura K, Yoshimaru K, Nakayama Y and Yoshikawa J.** The timing of the reflected wave in the ascending aortic pressure predicts restenosis after coronary stent placement. *Hypertens Res* 27:535-40, 2004.
- 28. Van Den Bos GC, Westerhof N, Elzinga G and Sipkema P.** Reflection in the systemic arterial system: Effects of aortic and carotid occlusion. *Cardiovasc Res* 10:565-573, 1976.
- 29. Westerhof N, Sipkema P, van den Bos GC and Elzinga G.** Forward and backward waves in the arterial system. *Cardiovasc Res* 6: 648-656, 1972.

Figure Captions

Figure 1: Schematic diagram showing the experimental set up. The latex tube is connected to the pump at its inlet through a polyurethane tube, and its exit is connected to the downstream reservoir through a hard plastic (Portex) connector and a polyurethane tube. The pump generates half a sinusoidal waveform in the forward direction. Pressure (P) and flow rate (Q) are measured at different sites along the elastic tube. The measured signals are collected digitally into a personal computer. Reservoir 1 provides the pump with water and ensures the system is free from bubbles, and reservoir 2 collects the fluid volume displaced by the pump. The dashed lines indicate the level of water in the tank and reservoirs.

Figure 2: The determination of the initial linear part of the PU-loop is shown in (a) and the pressure measured in a latex tube of 1m length and an 12mm diameter at 0.30m away from the reflection site is shown in (b). Wave intensity analysis is shown in (c). End of linear part, point R, corresponds well with the onset of reflected wave from wave intensity analysis, point M. Note that wave speed is determined by the average of the slopes over the period between points K and R.

Figure 3: Pressure and velocity measured in the ascending aorta during control conditions. The PU-loop is constructed and the initial linear part of the loop is determined using the new technique (a), pressure is plotted against time in (b) to translate the end of the linear part, point R, to time. Wave intensity analysis (c). Although the end of the initial linear part in the PU-loop (a) is not very obvious, the end of the linear part detected by the new method, point R, corresponds well with the onset of the reflected waves as determined using wave intensity analysis, point M.

Figure 4: Pressure and velocity measured in the ascending aorta during thoracic occlusion. The PU-loop is constructed and the initial linear part of the loop is determined using the new technique (a), pressure is plotted against time in (b) to translate the end of linear part, point R, to time. Wave intensity analysis is shown in (c). The end of the initial linear part in the PU-loop is more obvious in this example than in the example of **Figure 3** due to the earlier arrival of the reflected wave. Again, the end of the initial linear part of the loop, point R, corresponds well with the onset of the reflected waves as determined using wave intensity analysis, point M.

Figure 5: a) The relative arrival time determined using the PU-loop is compared with that determined using wave intensity analysis. The results of the new technique using the PU-loop correlates well with Wave Intensity Analysis ($r^2=0.83$, $p<.001$).

b) Bland-Altman plot showing the agreement between the two results. Dashed line is the mean difference between the two methods and the continuous lines indicate $\pm 2SD$ of the mean difference. Note that most of the data points fell within $\pm 2SD$ range, and the zero line fell within the confidence limits of the average, indicating no statistical significant difference between wave intensity analysis and the PU-loop methods for determining the arrival time of reflected waves.

Table 1: *The arrival time of reflected waves in tubes with different diameters*

Tube Diameter (mm)	Tube Wave speed (m/s)	Distance to Reflection Site (m)	Arrival Time of Reflected Waves (s)		
			f-t-f	PU-loop	WIA
			2L/c	R	M
4.00	6.77	0.30	0.0918	0.0960	0.0920
		0.40	0.1182	0.1140	0.1180
		0.50	0.1427	0.1400	0.1360
		mean	0.1176	0.1167	0.1153
		SD	0.0255	0.0221	0.0221
		% change	1		-1
8.00	5.66	0.30	0.1060	0.1160	0.1100
		0.40	0.1413	0.1240	0.1280
		0.50	0.1766	0.1780	0.1760
		mean	0.1413	0.1393	0.1380
		SD	0.0353	0.0337	0.0341
		% change	1		-1
16.00	3.80	0.30	0.1476	0.1360	0.1380
		0.40	0.2168	0.2160	0.2140
		0.50	0.2740	0.2880	0.2760
		mean	0.2128	0.2133	0.2093
		SD	0.0633	0.0760	0.0691
		% change	0.3		2

Values of mean \pm SD and the percentage change of the arrival time of reflected waves as determined using three methods; the new technique using the PU-loop method (point R, **Figure 3**), Foot-to-Foot method (f-t-f) and wave intensity analysis (WIA) using equation 1 (point M, **Figure 3**). The % change is calculated as the difference of the f-t-f, wave intensity methods, and the PU-loop method, compared to the PU-loop method.

Table 2: *A comparison between wave speeds determined using the PU-loop algorithm and that determined by eye.*

Dog no.	Wave speed [m/s]		
	c_1	c_2	$(c_1-c_2)/c_1$ [%]
1	4.67	4.60	1.6
2	8.70	8.18	6.4
3	4.25	4.22	0.8
4	4.83	4.82	0.1
5	4.38	4.23	3.4
6	9.65	9.20	4.9
7	8.03	7.79	3.0
8	5.52	5.42	2.0
9	5.87	5.91	-0.7
10	5.60	5.53	1.2
12	7.01	6.85	2.2
Average	6.23	6.07	2.6

Wave speeds determined using the PU-loop algorithm, c_1 , and that determined by eye, c_2 . For each method, the wave speed is the average of the entire wave speeds measured for all of the interventions. The global average of the percentage difference between the two techniques is 2.6%.

Figure 1

[Click here to download colour figure: Figure 1.doc](#)

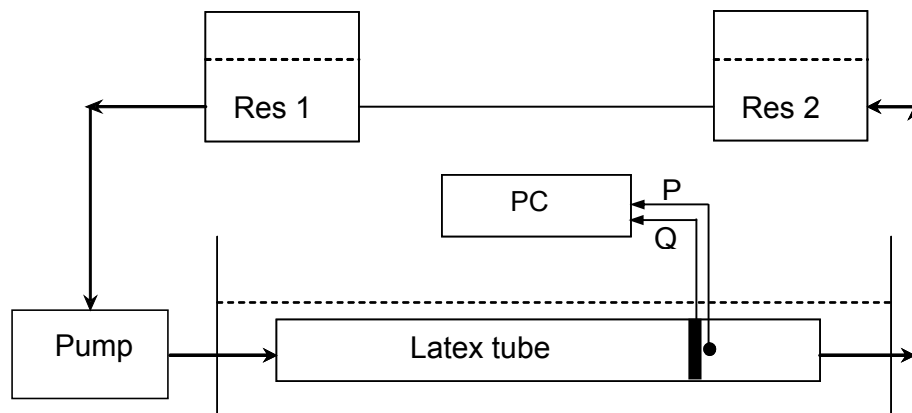


Figure 1: Schematic diagram showing the experimental set up. The latex tube is connected to the pump at its inlet through a polyurethane tube, and its exit is connected to the downstream reservoir through a hard plastic (Portex) connector and a polyurethane tube. The pump generates half a sinusoidal waveform in the forward direction. Pressure (P) and flow rate (Q) are measured simultaneously at different sites along the elastic tube. The measured signals are collected digitally into a personal computer. Reservoir 1 provides the pump with water and ensures the system is free from bubbles, and reservoir 2 collects the fluid volume displaced by the pump. The dashed lines indicate the level of water in the tank and reservoirs.

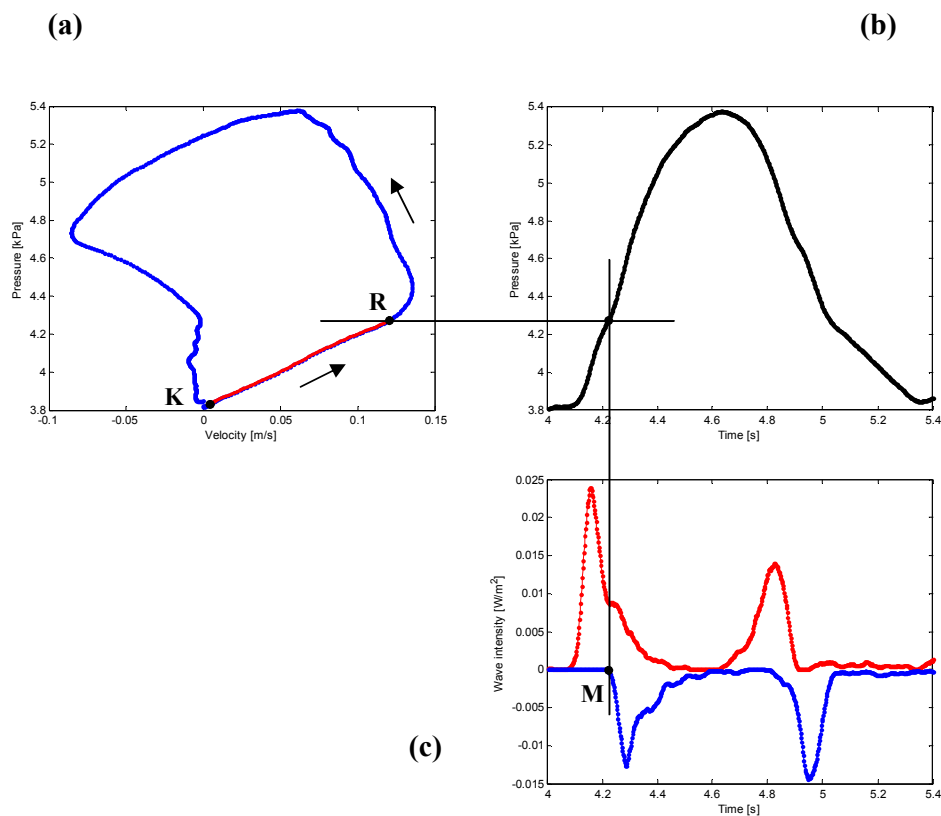
Figure 2[Click here to download colour figure: Figure 2.doc](#)

Figure 2: The determination of the initial linear part of the PU-loop is shown in (a) and the arrows indicate the direction of the loop. The pressure measured in a latex tube of 1m length and 12mm diameter at 0.30m away from the reflection site is shown in (b). Wave intensity analysis is shown in (c). End of linear part, point R, corresponds well with the onset of reflected wave from wave intensity analysis, point M. Note that wave speed is determined by the average of the slopes over the period between points K and R.

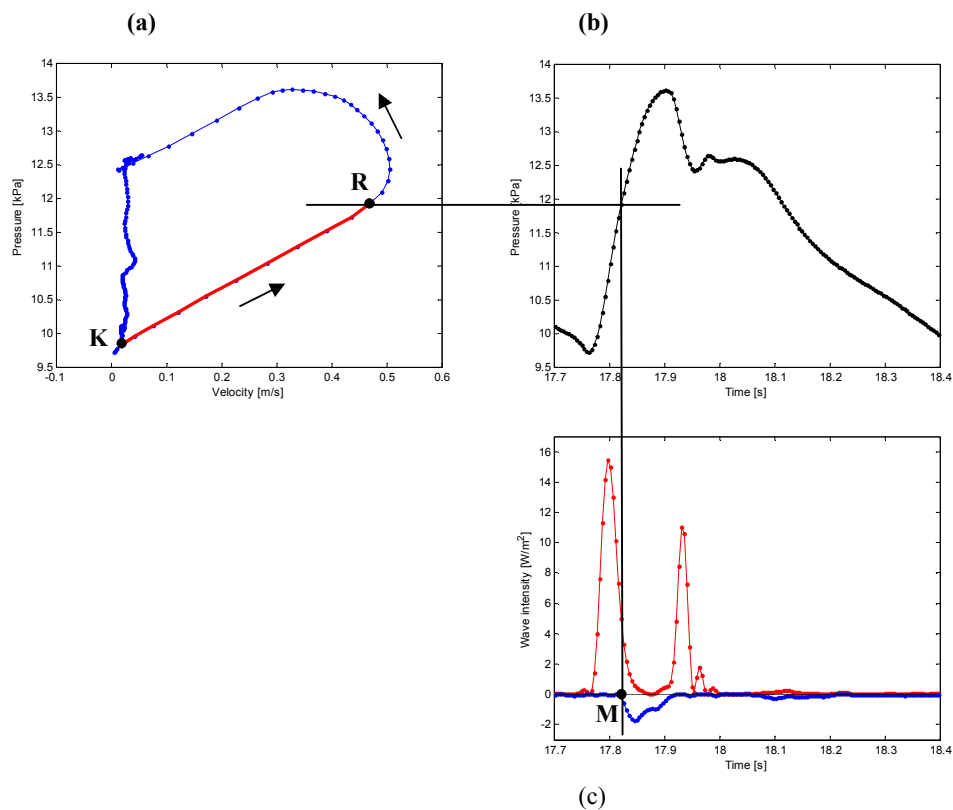


Figure 3: Pressure and velocity measured in the ascending aorta during control conditions. In (a) the PU-loop is constructed, the initial linear part of the loop is determined using the new technique and the arrows indicate the direction of the loop. The pressure is plotted against time in (b) to translate the end of the linear part, point R, to time. Wave intensity analysis is shown in (c). Although the end of the initial linear part in the PU-loop is not very obvious, it was detected by the new method, point R, which corresponds well with the onset of the reflected waves as determined using wave intensity analysis, point M.

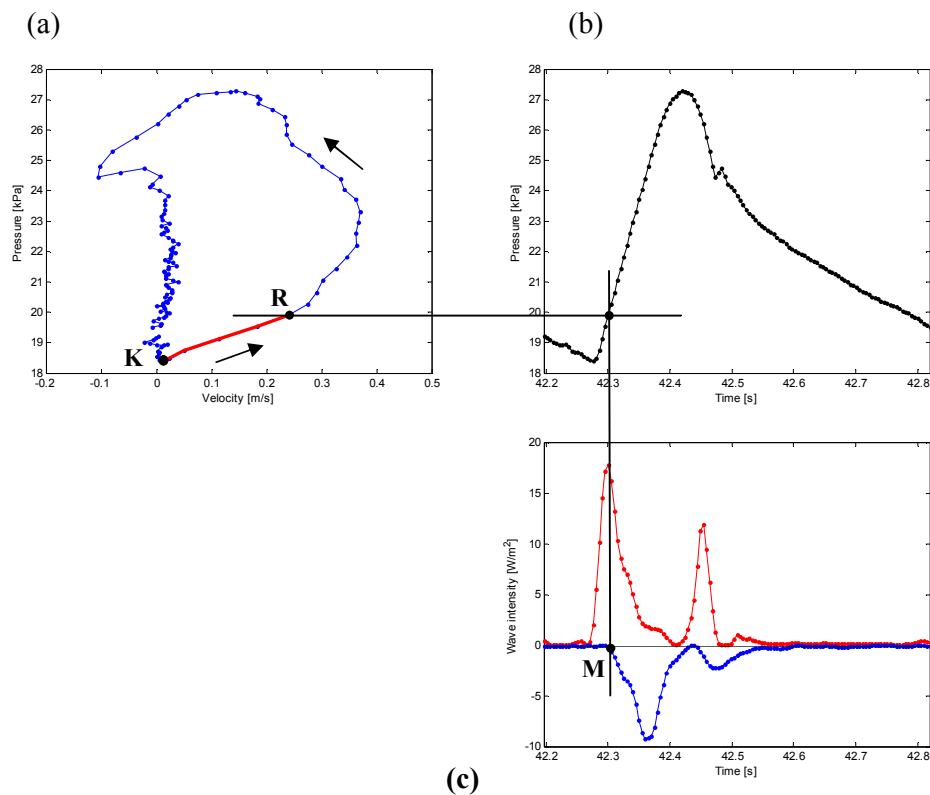
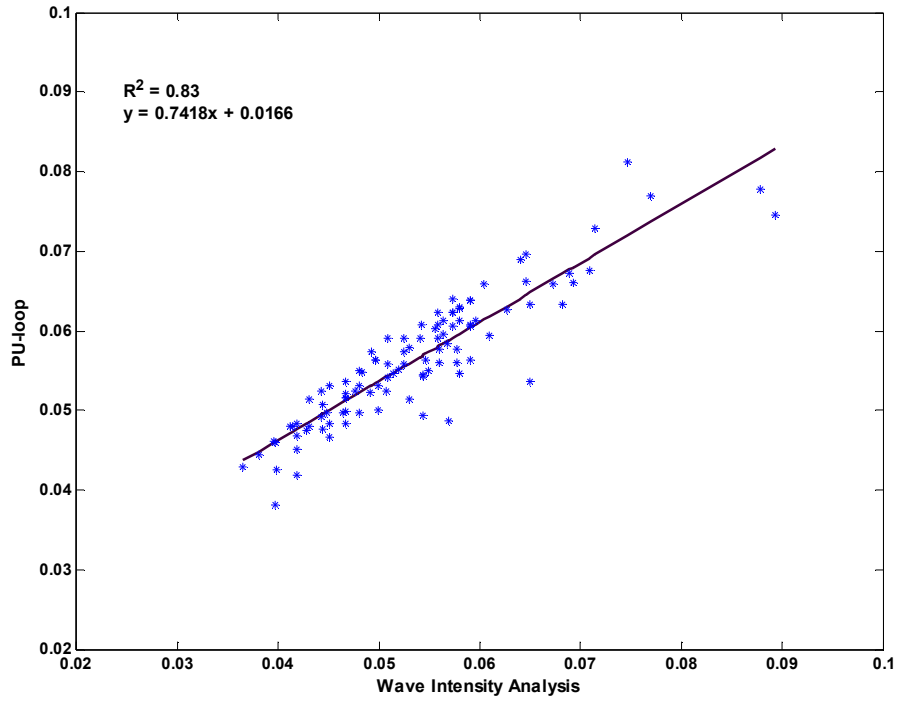


Figure 4: Pressure and velocity measured in the ascending aorta during thoracic occlusion. In (a) the PU-loop is constructed, the initial linear part of the loop is determined using the new technique and the arrows indicate the direction of the loop. The pressure is plotted against time in (b) to translate the end of linear part, point R, to time. Wave intensity analysis is shown in (c). The end of the initial linear part in the PU-loop is more obvious in this example than in the example of **Figure 3** due to the earlier arrival of the reflected wave. Similar to **Figure 3**, the end of the initial linear part of the loop, point R, corresponds well with the onset of the reflected waves as determined using wave intensity analysis, point M.

(a)



(b)

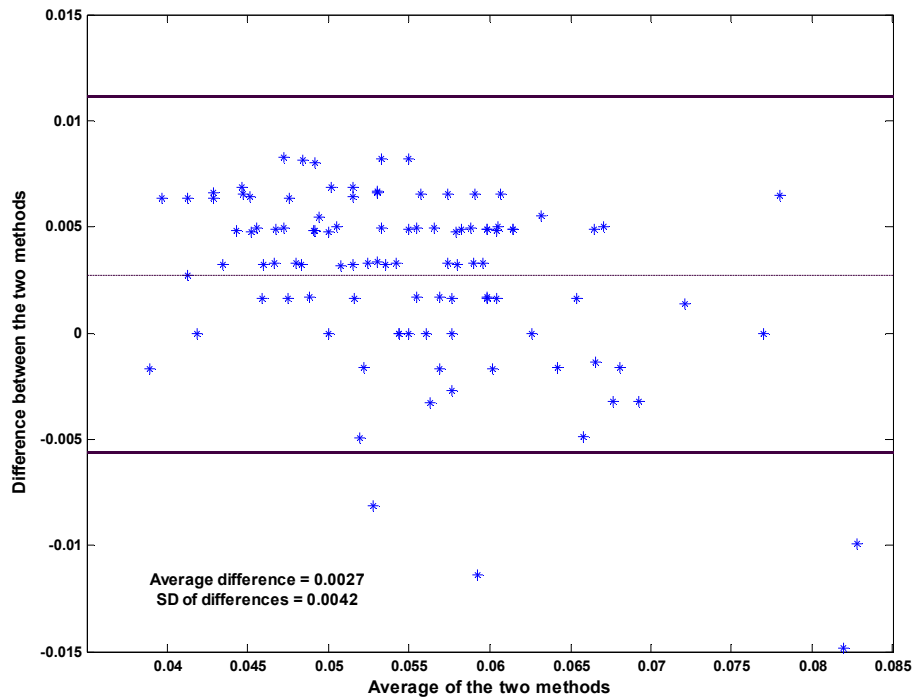


Figure 5: a) The relative arrival time determined using the PU-loop is compared with that determined using wave intensity analysis. The results of the new technique using the PU-loop correlates well with Wave Intensity Analysis ($r^2=0.83$, $p<.001$).

b) Bland-Altman plot showing the agreement between the two results. Dashed line is the mean difference between the two methods and the continuous lines indicate $\pm 2SD$ of the mean difference. Note that most of the data points fell within $\pm 2SD$ range, and the zero line fell within the confidence limits of the average, indicating no statistical significant difference between wave intensity analysis and the PU-loop methods for determining the arrival time of reflected waves.